




Understanding flood risk in urban environments: spatial analysis of building vulnerability and hazard areas in the Lisbon metropolitan area

Pedro Pinto Santos^{1,2}  · Susana Pereira^{1,3} · José Luís Zêzere^{1,2} · Eusébio Reis^{1,2} · Sérgio Cruz Oliveira^{1,2} · Ricardo A. C. Garcia^{1,2} · Tiago Miguel Ferreira⁴

Received: 26 December 2023 / Accepted: 30 May 2024
© The Author(s) 2024

Abstract

Climate change has brought about new risks while exacerbating existing ones, with floods now accounting for about 45% of global disasters. This trend indicates that the exposure to floods and resulting damages will continue to rise. This paper aims to contribute to the global efforts to enhance flood resilience in urban areas by introducing a physical vulnerability index for buildings in flood-prone urban areas and exploring its connection with flood hazard, as defined by the European Union Directive 2007/60/EC. An index-based methodology is proposed to assess the physical vulnerability of buildings to flooding, utilising the Portuguese Census and Georeferenced Buildings Database, collected on a nationwide scale. The physical vulnerability of buildings is evaluated in the context of the Lisbon metropolitan area (LMA) in Portugal, and the results are compared across different scales, contrasting flood hazard information for the entire LMA with the areas identified under the Flood Directive as having significant potential flood risk. Using cluster analysis, spatial patterns of flood risk are identified, highlighting areas where high flood depth and flood velocity overlap the high vulnerability of buildings. Lastly, potential adaptation paths are discussed, considering the diverse nature of the flood hazard and the lessons learnt from other flood events.

Keywords Flood risk · Urban areas · Physical vulnerability · Cluster analysis · Lisbon metropolitan area

1 Introduction

Climate change and geophysical events give rise to numerous disasters worldwide each year. Over the last two decades (from 2000 to 2022), data processing from EM-DAT reveals a staggering 8180 reposted disasters, with a striking 91% attributed to extreme weather events, with floods being the most prevalent, accounting for 45% of all disasters. The global impact of climate on flooding is evident through the exponential rise in flood occurrences from 1900 to 2021 (Fig. 1, left), and projections indicate a continuing upward trend (Alfieri et al. 2017).

Extended author information available on the last page of the article

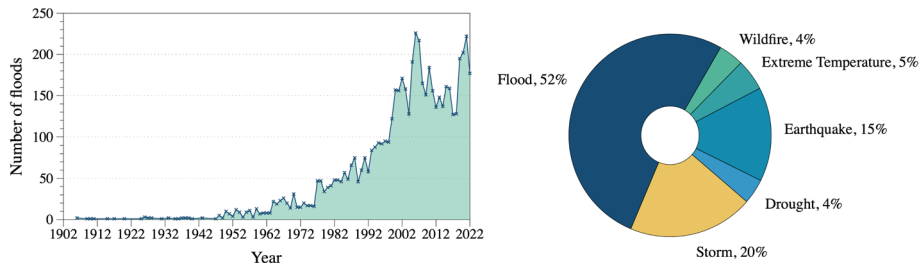


Fig. 1 Global frequency of floods per year (left); Proportion of economic losses from disasters in Europe between 2000 and 2021 (right). Data compiled from EM-DAT

In Europe alone, disasters have resulted in substantial economic losses, amounting to 281 billion US\$. Among these, floods constitute 52% of the damages, followed by storms (20%) and earthquakes (15%) (Fig. 1, right). Furthermore, studies estimate that exposure to floods and subsequent damage will triple by 2050 due to the increasing population and economic assets in flood-prone areas (Merz et al. 2021).

In response to these challenges, the European Union adopted Directive 2007/60/EC, providing a uniform flood risk assessment and management framework across its member states. Transposed into Portuguese national law by Decree-Law No. 115/2010, this framework introduces a series of challenges that make it necessary for robust scientific engagement. Central to the framework's objectives is the significance of flood risk maps, laying the foundation for Flood Risk Management Plans (FRMP). Crafting these plans entails addressing various challenges, including selecting the appropriate scale of analysis and establishing connections with land use and civil protection emergency plans. Hence, comprehensive flood risk studies play a vital role in bridging risk assessment and management processes within risk governance models (Aven and Renn 2010).

Traditional conceptual risk models comprise hazard, exposure, and vulnerability components (Miranda and Ferreira 2019). In the past, exposure was often implicitly incorporated without being considered an independent risk component (WBGU 2000; NATO 2006; Wisner et al. 2004). Recent flood risk studies within the context of climate change have generally treated exposure as a subcomponent of vulnerability (Choi 2019; Saber et al. 2020; Zahmatkesh and Karamouz 2017). However, certain risk models integrate societal and institutional dimensions, accounting for the capacity to cope with and adapt to threats (Marin-Ferrer et al. 2017). Interestingly, the Flood Directive 2007/60/EC does not explicitly incorporate the vulnerability concept, aiming for consistent applicability across EU countries.

Scale considerations play a crucial role in flood risk analysis. Different scales necessitate specific data and methodologies, with the analysis objectives influencing the chosen approaches (de Moel et al. 2015). Ensuring consistency and accuracy when comparing flood risk across scales remains a significant challenge. However, advancements in global datasets provided by Earth observation systems and improved computational capacities have alleviated some of the scale-related concerns, enabling more detailed flood risk analysis over broader areas (Shonkoff et al. 2015; Lindersson et al. 2021; Mazzoleni et al. 2021; Wing et al. 2018; Alfieri et al. 2018). The utilisation of flood hazard scenarios and vulnerability assessments in flood risk decision-making also varies across different scales. These analysis have been applied at various levels, ranging from

country-wide (Marin-Ferrer et al. 2017) and municipality-specific studies (Vojtek et al. 2023; Santos et al. 2022) to household-level investigations (Leal et al. 2021; Ferreira and Santos 2020). Each scale offers valuable insights and context-specific information to inform flood risk management strategies.

Assessing the vulnerability of elements at risk is a crucial factor in evaluating flood risk and potential damage. In recent years, various methods have been developed for this purpose. Physical vulnerability assessment methods can be categorised into three main groups, as highlighted by different authors (Nasiri et al. 2016; Huang et al. 2012): those based on disaster loss data, vulnerability curves, and index-based approaches.

Vulnerability functions, also known in the literature as damage functions, are mathematical functions that associate a specific flood parameter, typically water depth, with a relative amount of loss or an absolute monetary loss (Arrighi et al. 2020). Such functions are often developed based on expert judgment (Luino et al. 2012; Dottori et al. 2016; Arrighi et al. 2018) or derived from observed losses (Wagenaar et al. 2017; Carisi et al. 2018), while laboratory models have also been used recently for that purpose (e.g., Sturm et al. 2018; Mejía-Morales et al. 2023). Vulnerability curves represent the physical vulnerability of an asset, the intrinsic vulnerability of a typology of buildings, for example, and, therefore, they depend on the identification of key damage mechanisms. This aspect has been investigated by different authors, such as Laudan et al. (2017), who adopted a random forest approach to determine the importance of contributing variables (e.g., flood depth, flow direction, or year of construction), or Postacchini et al. (2019), who investigated the effect of flow characteristics and incidence angle on the flood impact on masonry buildings.

Unlike vulnerability functions, the primary aim of index-based vulnerability assessment approaches is not to quantify the losses but to compare the level of vulnerability of assets potentially exposed to flooding events. As discussed by Julià and Ferreira (2021), index-based vulnerability assessment approaches are particularly well-suited for flood vulnerability assessment in urban areas due to their holistic and integrative nature, and this is why several studies have focused on using this type of approach. For example, Mebarki et al. (2012) developed a method to estimate the probability of damage in masonry buildings based on flood depth and velocity. By analysing post-flood damage reports, they identified 14 physical vulnerability parameters and established an elliptical relationship between these parameters and flood depth. Stephenson and D'Ayala (2014) proposed an index-based methodology to assess the vulnerability of historical structures in the UK. This approach considered seven parameters, each assigned between 3 and 5 attributes, resulting in the calculation of a vulnerability index that aggregates the vulnerability ratings. Similarly, Gandini et al. (2018) introduced a holistic approach that considers both physical and social vulnerability indicators to assess the potential for historical buildings to be damaged by floods. Employing a multi-criteria approach and a decision tree, they obtained a unique vulnerability index on the building level. In line with this, (Miranda and Ferreira 2019) put forward a flood vulnerability assessment approach for historical centres, combining two indices related to exposure and sensitivity based on a comprehensive review of similar indicators. More recently, Ferreira and Santos (2020) expanded upon the approach of Miranda and Ferreira (2019) to generate physical vulnerability results. These results were then integrated with hazard data to produce flood risk maps for the Historic Centre of Guimarães, Portugal.

Building on the context outlined above, the main purpose of this paper is to explore the combined use of flood hazard and building vulnerability results to identify the urban blocks in the Lisbon metropolitan area (LMA), used here as a case study, where flood adaptation and mitigation are of utmost priority. A multi-criteria method is introduced in this work to

assess the physical vulnerability of buildings to floods, with the selection of variables, their classes, and weighting based on robust support from the scientific literature. The utility of this physical vulnerability index lies in the fact that the methodology was specifically tailored to capturing vulnerabilities specific to our study context, at a scale that is not frequently addressed, and used data that were not specifically gathered for that purpose. The ability to apply it to vast areas define it as appropriate for regional and local risk decision-making. The resulting characterisation is then correlated with two levels of flood hazard: a simplified measure of susceptibility for the entire LMA—following the geomorphological approach, which provides information applicable to extensive areas, addressing a broader temporal scale as it is based on past flood evidence—, and a detailed mapping of flood depths and velocities—following a hydrological-hydraulic approach—as mandated by the implementation of the Directive 2007/60/EC, which undergoes a cluster analysis.

2 The Lisbon metropolitan area case study

2.1 Geographical context

As mentioned earlier, the case study area is located within the geographical limits of the Lisbon metropolitan area (LMA), Portugal (Fig. 2).

It comprises 18 municipalities, with the country's capital, Lisbon, being the most populated among them. Covering an area of 3105 sq. km, the LMA is home to approximately 2.8 million residents. The population distribution is uneven, with concentrations along the coast in the municipalities of Cascais, Oeiras, Lisbon, Loures and V.F. Xira in the northern part of the LMA. In the southern LMA, besides Setúbal, the most populated areas face the Tagus estuary, including Almada, Seixal, Barreiro and Montijo. Sintra and Odivelas also have substantial built-up areas, with some occupying parts of the valleys of small streams.

2.2 General characteristics of the built environment

The built environment of the LMA comprises a diverse mix of building typologies. Urban areas are mainly composed of traditional unreinforced masonry (URM) buildings and modern reinforced concrete (RC) structures. RC buildings are the predominant type, accounting for 65% of the building stock in the LMA, while URM buildings constitute about 34%. The remaining 1% includes other types of structures, such as steel and timber constructions. Residential use dominates the majority of buildings, comprising 91%, with 8% serving mixed (commercial and residential) purposes, and the remaining 1% being dedicated solely to commercial use.

Within the URM category, four main typologies have been identified in the LMA (Simões et al. 2017). 'Pre-Pombalino' buildings, which date back to the period before the 1755 Lisbon Earthquake. They feature irregular geometry and have up to four storeys with poor-quality masonry. 'Pombalino' buildings, constructed after the 1755 Earthquake until 1870, are characterised by structural regularity and can have up to five storeys with mixed usage. 'Gaioleiro' buildings, built between 1870 and 1930, can have up to six stories and lower construction quality. 'Placa' buildings, typically constructed between 1930 and 1960, combine masonry walls with reinforced concrete elements.

In terms of RC buildings, their main typologies are distinguished by the analysis of the buildings' period of construction and the number of storeys (Xofi et al. 2023).

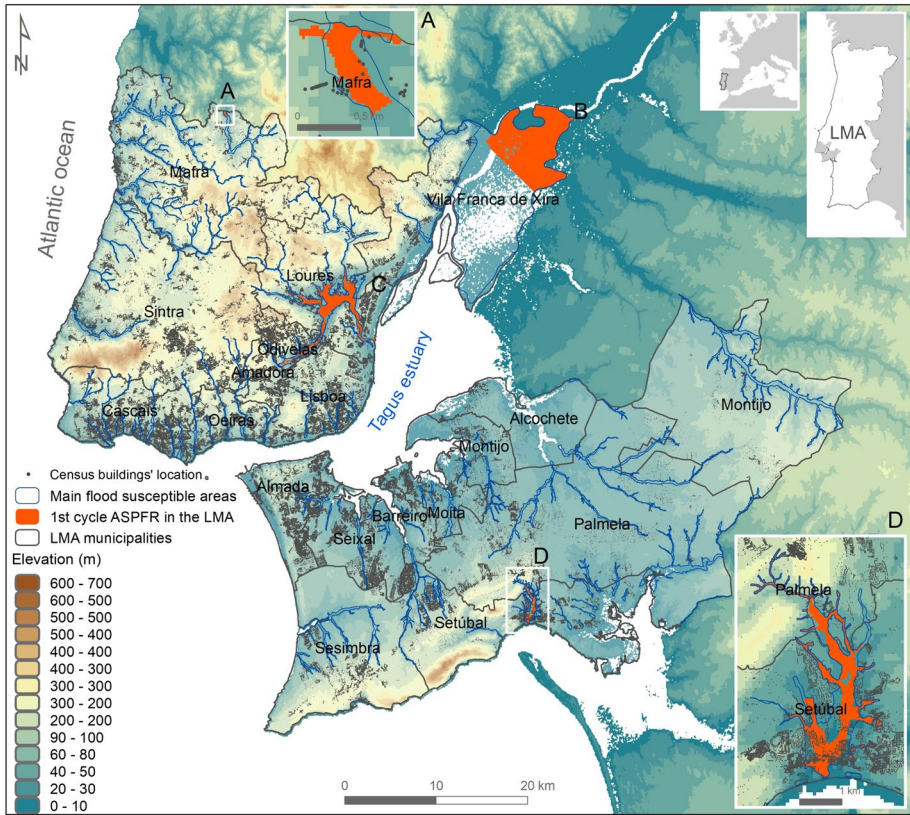


Fig. 2 Flood susceptibility in the LMA and in the Flood’s Directive areas (1st cycle) of significant potential flood risk. Torres Vedras (A), Tagus floodplain (B), Loures and Odivelas (C) and Setúbal (D)

‘Low-rise RC frame buildings’ (pre-code, i.e., before 1958) are typically up to three storeys. ‘Medium-rise RC frame buildings’ (mid-code, i.e., between 1958 and 1983) usually feature up to six storeys. Finally, ‘high-rise RC frame, wall, and dual systems buildings’ (post-code, i.e., after 1983) are typically more than seven storeys.

2.3 Flood types and flood hazard

The areas of significant potential flood risk (ASPFR) were defined considering riverine floods (flash and progressive) and the particular type of urban flooding, quite often associated with flash floods in the urban context. Coastal flooding is, therefore, excluded from this analysis although it is relevant in the LMA, particularly in the municipalities bathed by the Tagus estuary, and in Setúbal bathed by the Sado estuary.

In the LMA, progressive floods are observed in the Tagus River. With the regularization of flow regimes caused by dams in the last decades, the frequency and, specifically, the magnitude of this type of flood has been reduced. 1978 (11,500 m³/s), 1979 (15,000 m³/s) and 1989 (10,900 m³/s) are the years of the highest floods in the last 50 years, as measured c. 30 km upstream from the LMA boundary—Vila Franca de Xira—along the Tagus river (Loureiro 2009). Progressive floods with lower magnitude occurred in 2013, 2019

and 2022. The human impacts caused by this type of flood are essentially the evacuation and temporary displacement of residents (Zêzere et al. 2014).

Most of the municipalities in the LMA are affected by flash floods generated in small basins, which drain directly into the ocean or into the estuaries of the Tagus and Sado rivers. In addition to the small size of the catchments it should be noted that the catchments cross densely urbanized areas, thus exhibiting a high degree of soil imperviousness, which results in short times to peak (Leal and Ramos 2013). Traditionally characterized by a higher number of fatalities in comparison with progressive floods—e.g. the catastrophic flash floods of 1967 and 1983, in response to rainfall intensities of 137 and 164 mm/day, respectively (Zêzere et al. 2015)—the trend of the last decades shows a reduction in the number of lives lost (Pereira et al. 2016).

3 Data and methods

Input data regarding the three risk modules—hazard, exposure and buildings’ physical vulnerability—are collected and processed at two levels of analysis: the entire LMA and the critical areas defined in the Flood’s Directive. Flood hazard is assessed for the entire LMA using a geomorphological approach, while hydrologic-hydraulic modeling applied to the Directives’ areas allowed for a classification of buildings based on cluster analysis (Fig. 3).

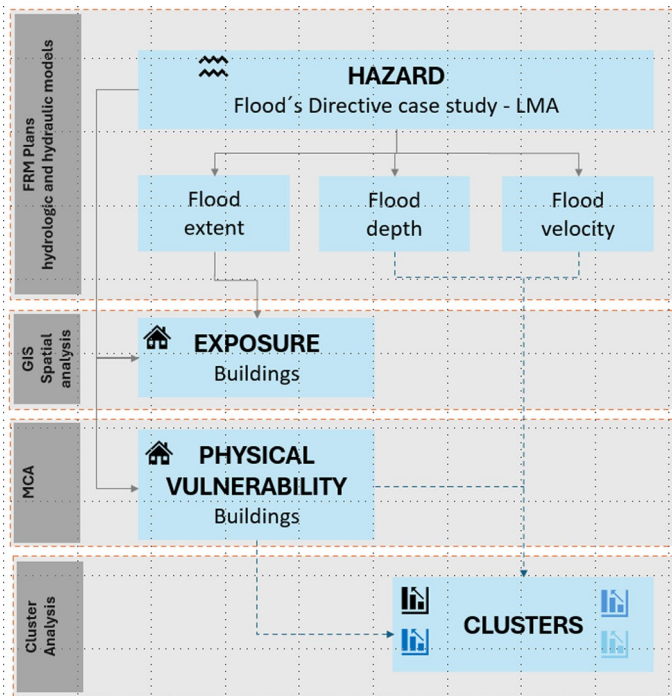


Fig. 3 Methodological flowchart followed in this study: linkages between the hazard, exposure and physical vulnerability modules and the cluster classification in the most critical areas

Given that the information regarding the hazard does not constitute an output specifically prepared for the purpose of this article, the data and methods are described below but are not considered separately in the results section.

The following sections describe in detail the used data and methodology.

3.1 Hazard module

3.1.1 Flood susceptibility in the LMA

A thorough analysis of the susceptibility to riverine flooding was conducted for the entire LMA. This mapping was carried out by the authors in 2020 in the scope of the elaboration of the Regional Spatial Plan for the West and Tagus Valley region (PROT-OVT). It follows two sequential steps.

The first step consists of identifying the reaches from the entire river network that are more prone to overbanking, i.e., to initiate a flooding condition at a given section of the river network. For that purpose, the approach first presented by Reis (2011), and later explored elsewhere, but particularly by Jacinto et al. (2015), Santos et al. (2019) and Santos and Reis (2018), was applied. This approach considers, at each location of the basin, the cumulative role performed by the entire upstream area concerning a set of flood conditioning factors: the flow accumulation, the slope and the relative permeability of the soil and underground substrate. The output is a classification of the drainage network in susceptibility classes, for which a fixed threshold is defined, retaining only the most susceptible reaches.

The second step takes as input the drainage network with the highest susceptibility resulting from the first step (linear data) and—contiguously to it—defines the areas of flood susceptibility (polygonal data). This was performed by following the hydro-geomorphologic principles developed by Díez-Herrero et al. (2009) and Ballais et al. (2011). The disposition and types and landforms and deposits are analyzed based on remote sensing imagery and topographic maps at a 1:25,000 scale. False color imagery and vegetation types are also accounted for in the delimitation of the maximum flood extent, from a hydro-geomorphologic perspective. It provides, in general, a conservative but validated approach, because it assumes that locations near the edge of the floodplain, where there is past evidence of flooding, are susceptible of testifying flooding in the present and future.

3.1.2 Flood hazard in the flood's directive areas

The detailed flood hazard assessment was conducted under the Flood's Directive and covers four areas of significant potential flood risk (ASPFR) in the LMA: Torres Vedras (A) Tagus floodplain (B), Loures and Odivelas (C) and Setúbal (D) (Fig. 2). From the existing flood hazard maps, the 100-yr return period was chosen. In the downstream section of each ASPFR, the peak flows are respectively 470 m³/s, 14,600 m³/s, 1017 m³/s and 137 m³/s.

The Torres Vedras ASPFR comprises a small section of the Pequeno River, a tributary of the Sizandro basin. It is a flash flood-type ASPFR with 15.2 sq. km, of which only 0.2 sq. km is within the LMA, in Mafra municipality. As said, Tagus's ASPFR is the only one where slow-onset flooding processes occur. It covers an area of 483.3 sq. km, although only 47.6 sq. km is part of the LMA (in the V.F. Xira municipality). Even so, it is by far the largest ASPFR in the study area. The Loures and Odivelas area comprises a sector of the Trancão River, a Tagus River tributary. Its 14.0 sq. km covers the municipalities of Loures

(12.4 sq. km), Odivelas (1.5 sq. km) and V.F. Xira (0.1 sq. km). The Setúbal ASPFR is considered the fluvial type, although the existence of tidal variations due to the proximity to the ocean affects only the southern sector of the area. It covers 2.4 sq. km, distributed by Palmela (0.5 sq. km) and Setúbal (1.9 sq. km) municipalities.

For the same fluvial reaches of the ASPFR, the geomorphological approach provides greater susceptible flood areas: Torres Vedras (0.28 sq. km), Tagus (50.6 sq. km), Loures and Odivelas (20.2 sq.km) and Setúbal (3.4 sq. km).

According to the scientific reports that support the elaboration of the Flood Risk Management Plans (FRMP) of the 1st cycle, the flood peaks were estimated with (1) statistical methods where long and consistent data series of maximum annual peak flows existed, (2) using the rainfall-runoff MOHID Land hydrologic model where flow data was inexistent. The hydraulic model was run with the same MOHID Land model, which recurs to 1D modelling on the channel network and 2D modelling on the overland flow. While the free surface flow is solved with the Saint–Venant equation, the sub-surface flow modelling recurs to the Richards equation (APA 2014). The outputs of the flood hazard assessment of the Flood’s Directive used in this paper are the flood extent—from which the affected buildings are identified—, and the flood depths and velocities.

3.2 Exposure module

The 2011 Portuguese Census includes geographical information about the location and characteristics of all the buildings that—partly or entirely—include a residential function, which is named the georeferenced buildings database (BGE). The two selected variables for expressing exposure are the number of buildings with a residential function and the number of inhabitants *per* building. This second variable is the result of an estimation based on the dasymetric distribution of the residents in the smallest polygonal statistical unit, the sub-section, according to the number of residential households in the building, accounting for the vacant households (Garcia et al. 2016).

3.3 Physical vulnerability module

The assessment of the physical vulnerability of the buildings relies on data sourced from the 2011 Portuguese Census, specifically the BGE. This dataset encompasses 14 variables detailing relevant characteristics of the residential buildings, including construction materials, structural systems, and conservation state. Out of these 14 variables, seven were selected to gauge physical vulnerability, forming the basis for calculating a vulnerability indicator. Denoted as Phys.V., this indicator is derived by computing the weighted sum of the parameters outlined in Table 1, as shown in Eq. 1. To aid in result interpretation and subsequent integration with hazard and exposure data, Phys.V. scores are normalised to a scale between 0 and 100 using the min–max method.

$$\text{Phys.V.} = P1 \times W_{p1} + P2 \times W_{p2} + P3 \times W_{p3} + P4 \times W_{p4} + P5 \times W_{p5} + P6 \times W_{p6} + P7 \times W_{p7} \quad (1)$$

In Eq. 1, C_{vi} represents the vulnerability class assigned to each parameter, P_i , and W_{pi} is the weight assigned to that parameter. The vulnerability classes, C_{vi} , and the weights, W_{pi} , associated with each physical vulnerability parameter, P_i , are given in Table 1. According to this classification, the higher the class (from A to D), the higher the level of physical vulnerability of the building to that aspect or feature.

Table 1 Physical vulnerability parameters, weights and classes

Phys.V. parameters, P_i	Vulnerability class, C_{vi}				Weight, W_{pi}
	A (10)	B (40)	C (70)	D (100)	
P1 Period of construction	1981–2011	1961–1980	1919–1960	Before 1919	1.5
P2 Number of storeys	1 Storey	2 Storeys	4 Storeys	4 + Storeys	1.0
P3 Cladding material	Tile/ceramic	Stone	Wood/glass	Traditional plaster	1.5
P4 Structural system	RC	URM+RC	URM+timber	Adobe	1.0
P5 Soil and lithological context	Hard rock	Weathered rock	Sandy deposits	Alluvial deposits	1.0
P6 Building exposure	Clustered	–	–	Isolated	0.5
P7 Condition	Very good	Good	Poor	Very poor	1.5

It is important to note that the parameters used in this work were defined after a comprehensive analysis of similar indicators available in the literature, which have been utilised by various authors to assess similar building typologies and structural characteristics under equivalent assessment conditions. Table 2 provides a comprehensive overview of the selected parameters, along with their theoretical and empirical foundations that guide their role in either increasing or decreasing the vulnerability of buildings.

Regarding the vulnerability classes, C_{vi} , and the weights, W_{pi} , they were determined based on relevant literature sources (e.g., Stephenson and D’Ayala 2014; Miranda and Ferreira 2019) and expert opinion. It is also worth noting that since the primary aim of the vulnerability analysis presented in this work is to hierarchize the level of physical vulnerability among different clusters of buildings rather than to estimate damages and losses, the validation of the correspondence between these indicators and actual discrete levels of physical vulnerability is not critical.

3.4 Cluster analysis

A clustering classification method was applied with the purpose of better characterizing and understanding the relations between the flood hazard’s depth and velocity and the physical vulnerability of buildings, in support of spatial and emergency planning. The input variables in the cluster analysis are the physical vulnerability of buildings, flood depth and flood velocity *per* building. As the Census buildings are represented by a point-type geometric feature, a 10-m radius was applied to select the buildings to be considered in the cluster analysis. The mean of flood depth and flood velocity of the cells touched by that radius was calculated and assigned to the respective building.

The clusters of buildings were obtained by running first a Two-Step Cluster Analysis in SPSS[®], testing 2–10 clustering solutions with Schwarz’s Bayesian Criterion (BIC). After applying the above spatial filter, the statistical individuals are the 2766 buildings located in ASPFR.

Given that the Schwarz’s Bayesian Criterion (BIC) is continuously decreasing as the number of clusters increases, the decision to opt for the 4 clusters was based on the analysis of the silhouette plot, and the balance between the Ratio of Distance Measures (the highest in the 4-cluster solution, 1.791) (Table 3) and expert opinion considering the diversity of combinations of input variables expressed by the clusters.

Table 2 Parameters for the assessment of the physical vulnerability of buildings to floods

Phys.V. parameters	Rationale	Source
P1 Period of construction	Building age is a commonly used indicator for construction techniques and materials but ranks lower in flood vulnerability	Agliata et al. (2021), Pereira et al. (2020), Leal et al. (2021), Kappes et al. (2012)
P2 Number of storeys*	Taller buildings may have deeper foundations, making them less prone to flood damage, but can also be more susceptible to differential settlements due to poor ground conditions and shallow footings	Agliata et al. (2021), Pereira et al. (2020), Kappes et al. (2012), Miranda and Ferreira (2019), Stephenson and D'Ayala (2014), D'Ayala et al. (2020)
P3 External cladding material	The absorption of the cladding material directly affects the building fabric, influencing its vulnerability to floods	Leal et al. (2021), Kappes et al. (2012)
P4 Structural system	The material of the structural system has an indirect impact on the building's performance during flooding compared to P3 and P7	Leal et al. (2021), Kappes et al. (2012)
P5 Soil and lithological context	The soil and lithological context control soil saturation and erodibility during flooding and, in accordance, with the building foundation choices and the structural system. This indicator ranks less significant in flood vulnerability due to higher uncertainty compared to other indicators	Empirical data
P6 Building exposure	Isolated buildings are more prone to collapse, while non-isolated buildings are less vulnerable. However, this indicator ranks less significant in flood vulnerability due to higher uncertainty compared to other indicators	Agliata et al. (2021), Kappes et al. (2012)
P7 Condition**	The existing condition of a building can be affected first by flooding, especially considering the building fabric material (parameter P3), making it more prone to damage	Agliata et al. (2021), Kappes et al. (2012), Silva and Pereira (2014), Stephenson and D'Ayala (2014), D'Ayala et al. (2020)

*Most debated indicator as experts interpret and use it differently depending on the building feature and behaviour they intend to describe with it (Agliata et al. 2021)

**Most used indicator reflecting the capacity of construction to resist flood impact

Table 3 Auto-clustering table resulting from the two-step cluster analysis, using physical vulnerability, flood depth and velocity for the buildings within ASPFR

Number of clusters	Schwarz's Bayesian criteria (BIC)	BIC change	Ratio of BIC changes	Ratio of distance measures
1	5797.786			
2	4361.895	- 1435.891	1.000	1.661
3	3516.506	- 845.389	0.589	1.623
4	3014.033	- 502.473	0.350	1.791
5	2754.487	- 259.546	0.181	1.407
6	2583.726	- 170.761	0.119	1.031
7	2419.629	- 164.097	0.114	1.030
8	2261.601	- 158.028	0.110	1.389
9	2161.149	- 100.452	0.070	1.105
10	2074.769	- 86.379	0.060	1.308

4 Results

4.1 Exposure of buildings and population

The results of this research consist of the analysis of exposure and buildings' physical vulnerability under the two flood hazard scenarios: the one elaborated for the entire LMA (applying the geomorphological approach, and the one for the Flood's Directive ASPFR, which cover 4 areas).

The flood susceptibility mapping, as carried out during the elaboration of the PROT-OVT, identifies 269.6 sq.km of susceptible areas, 8.7% of LMA (cf. also Fig. 4): 144.3 sq. km correspond to progressive floods, 122.1 sq. km to flash floods and 3.2 sq. km to flooding associated with natural lagoons and dam reservoirs. V.F Xira is by far the municipality with most of its area under flood susceptibility (149 sq. km, corresponding to 60% of its surface discounting intertidal areas). 10,206 residential buildings are located in the susceptible area, from a total of 449,573 in the LMA (2.3%), home of 72,676 inhabitants (2.6% of the total LMA). The municipalities most potentially affected by flooding are Lisbon (1813 buildings in 3.2% of the susceptible area), Odivelas (1314 buildings in 11.6%) and Setúbal (1781 buildings in 5.2% of the susceptible area) (Table 4).

Focusing on the four ASPFR of the Flood's Directive, the hydraulically modelled flood-prone areas express small figures of exposed elements: as an example, from Table 4, the Setúbal ASPFR accounts 1411 buildings (62 plus 1349 buildings from the Palmela and Setúbal municipalities). For the same fluvial reaches, the LMA's geomorphological approach sums 1787 buildings. This is observed in the other ASPFR as well, and is explained by the fact that the geomorphological methods express past sedimentological and morphological evidence of floods, in a more conservative perspective, the one of the maximum probable flood, to which it is not possible to assign an exact return period.

In resume, the area with the most exposed buildings is Setúbal (1411, and 11,293 inhabitants) followed by Loures and Odivelas (1317, and 11,432 inhabitants), Tagus (33, and 39 inhabitants) and Torres Vedras, in the Mafra municipality (5 buildings, and 11 inhabitants).

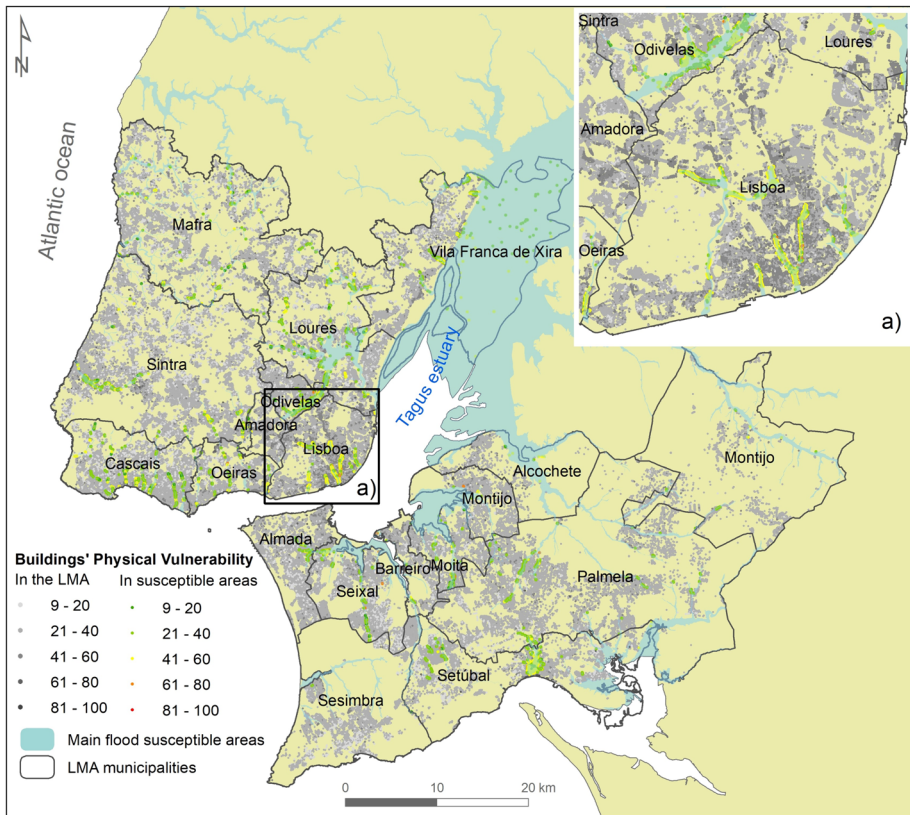


Fig. 4 Physical vulnerability of buildings to flooding in the LMA and in susceptible areas

4.2 Physical vulnerability of buildings

4.2.1 In the Lisbon metropolitan area

In the LMA's geomorphologically identified flood susceptible areas, the mean Phys. V. values is 35, with a minimum mean of 23 in Amadora municipality and a maximum in Lisbon (50). In the other two of the three most exposed municipalities, the Phys. V. value is also above the mean: 40 in Odivelas and 44 in Setúbal, which is a concerning fact for the medium-term risk adaptation and reduction and short-term emergency planning and response.

Amadora and Sesimbra stand out as municipalities with lower exposure (28 in 13,719, and 5 in 20,436 buildings, respectively), and low Phys. V (mean values of 23 and 25, respectively), despite Sesimbra featuring 4.5% of the territory under flood susceptibility.

Table 4 Cross-scale perspective of exposure to flood in the LMA, and particularly in the four Flood's Directive critical areas comparing the flood mapping from the hydro-logic-hydraulic and the geomorphological approaches

Municipalities	LMA flood susceptible areas (for all the municipality area)									
	LMA					Flood Directive's critical areas				
	Bldgs (abs.)	Inhabs (abs.)	Bldgs (abs.)	Bldgs (%)	Inhabs (abs.)	Inhabs (%)	Directive's hydro-logic-hazard	Geomorphological susceptibility	Directive's hydro-logic-hazard	Geomorphological susceptibility
Alcochete	4575	17,740	12	0.3	23	0.13	-	-	-	-
Almada	34,343	173,906	194	0.6	888	0.51	-	-	-	-
Amadora	13,719	175,440	28	0.2	227	0.13	-	-	-	-
Barreiro	11,024	78,744	46	0.4	190	0.24	-	-	-	-
Cascais	43,650	207,187	780	1.8	3305	1.60	-	-	-	-
Lisboa	52,546	542,917	1813	3.5	17,674	3.26	-	-	-	-
Loures*	31,144	206,025	992	3.2	3505	1.70	387	1716	651	2717
Mafra	28,008	77,452	255	0.9	524	0.68	5	11	12	26
Moita	12,408	66,091	124	1.0	236	0.36	-	-	-	-
Montijo	13,025	51,777	39	0.3	66	0.13	-	-	-	-
Odivelas*	16,371	145,707	1314	8.0	13,419	9.21	930	9716	1314	13,419
Oeiras	18,247	172,478	341	1.9	2729	1.58	-	-	-	-
Palmela	21,642	63,144	336	1.6	877	1.39	62	145	66	152
Seixal	30,145	159,261	533	1.8	4691	2.95	-	-	-	-
Sesimbra	20,436	49,738	5	0.0	5	0.01	-	-	-	-
Setúbal	24,320	121,061	1781	7.3	14,485	11.97	1349	11,148	1787	15,605
Sintra	56,917	378,733	577	1.0	5311	1.40	-	-	-	-
V. F. Xira	17,053	137,509	1036	6.1	4521	3.29	33	39	147	374
LMA	449,573	2,824,910	10,206	2.3	72,676	2.6	2766	22,775	-	-

*The Flood Directive's critical area Loures/Odivelas covers partially these two municipalities

4.2.2 In the flood's directive ASPFR

The LMA's ASPFR of the Flood's Directive with the highest mean Phys. V. is Setúbal (39.9), followed by Loures and Odivelas (35.4), Tagus floodplain (34.0) and Torres Vedras (33.6) which, considering the amplitude of scores (from 13 to 79), is close to the mean Phys. V. of the entire susceptible LMA's areas (35.0).

By combining Phys. V. and hazard components, classification in clusters contributes to better predict how risk drivers may perform during flood events. Each of the exposed buildings located in the Flood Directive's critical areas was categorized in clusters as follows: cluster 1, which includes only 8 buildings, cluster 2 including 565, cluster 3 including 906 and cluster 4 including 1287 buildings. As an anticipated summary of the cluster characteristics, to be further detailed, it can be drawn that cluster 1 represents the buildings where physical vulnerability is in general very high. Cluster 2 expresses the buildings where the hazard is high, and Phys. V. is medium. Cluster 3 aggregates the buildings in the safest context—the lowest mean physical vulnerability, and low hazard (it has the lowest mean flood depths). Finally, cluster 4 represents intermediate contexts in both Phys. V. and flood hazard.

Buildings exposed to the highest flow velocities (Fig. 5) are found in the Loures and Odivelas ASPFR (2.6 m/s) and Setúbal (1.1 m/s) due to their proximity to the main channel of these ASPFR. On average, the buildings exposed to flooding are subject to

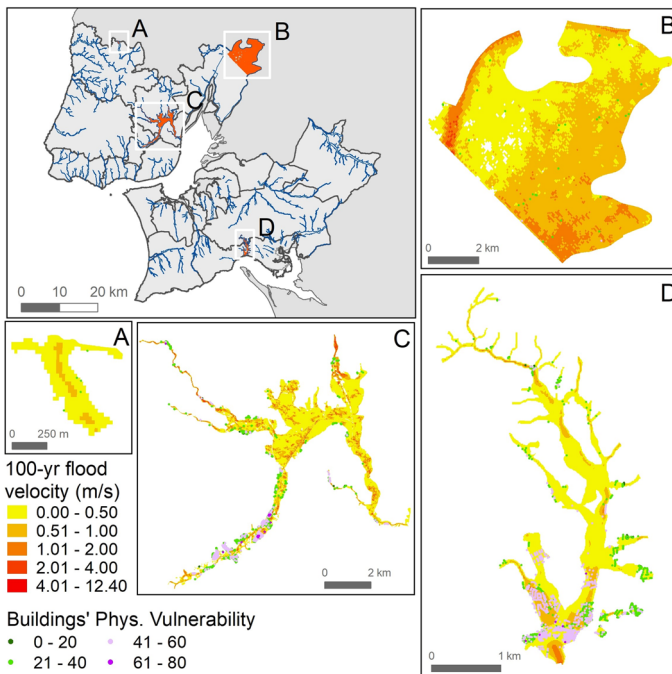


Fig. 5 The spatial relation between flood velocity and physical vulnerability of buildings to flooding in the Flood Directive's areas of significant potential flood risk in the LMA: Torres Vedras (A), Tagus floodplain (B), Loures and Odivelas (C) and Setúbal (D)

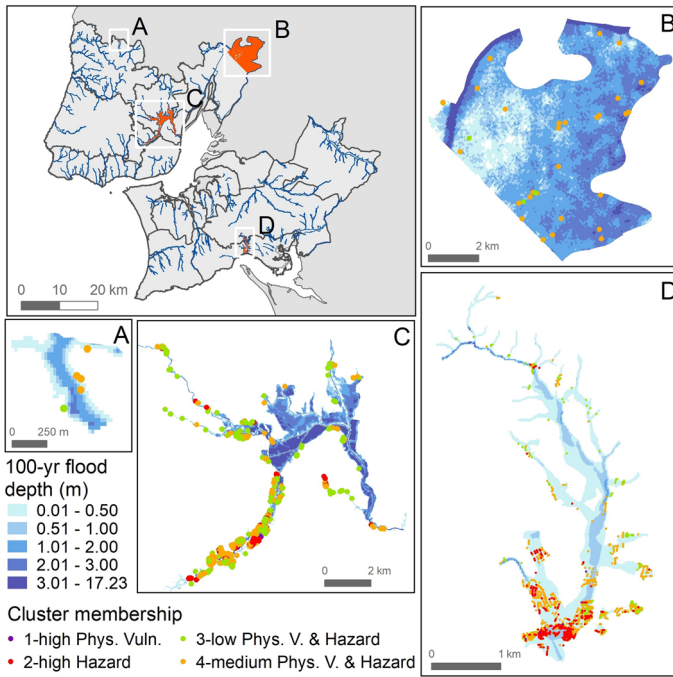


Fig. 6 The spatial relation between flood depth and cluster membership of buildings to flooding in the Flood Directive’s areas of significant potential flood risk in the LMA: Torres Vedras (A), Tagus floodplain (B), Loures and Odivelas (C) and Setúbal (D)

velocities of 0.6 m/s in the Tagus ASPFR, 0.3 in Setúbal, 0.2 in Loures and Odivelas and 0.1 m/s in Torres Vedras.

In the hazard variables, mean flood depths are higher in cluster 2, with 0.5 m, while mean flow velocity (m/s) is higher in clusters 2 and 4 (Figs. 6, 7B). The highest mean flood depth and flow velocity are found in the Tagus floodplain (1.5 m and 0.6 m/s, respectively), followed by Loures and Odivelas (0.8 m and 0.3 m/s, respectively).

In the exposure variables (mean number of inhabitants and mean number of households), clusters 2 and 4 stand out with the highest mean values (Fig. 7A). This finding is interesting, as the three variables used in the cluster analysis don’t include the number of inhabitants, but there is an evident distinction of clusters 1 and 3 from the others on this regard.

Summing up all the inhabitants and households in each cluster, cluster 4 stands out with 8247 exposed households and 14,885 exposed inhabitants. A total of 22,776 exposed inhabitants are found in the four ASPFR, but Loures and Odivelas comprise 50.2% and Setúbal 49.6% of the exposed inhabitants. The same concentration in these two study areas is found in the total exposed households (12,815) with 51% in Setúbal and 47.6% in Loures and Odivelas.

When the analysis is focused on the parameters of Phys. V of buildings exposed to floods, cluster 1 presents the highest mean values for all parameters (P1, P2, P3, P4, P5, P6 and P7) (Fig. 7C), and the highest Phys. V. index (75.5), concentrated in the critical areas of Setúbal, Loures and Odivelas (Fig. 8).

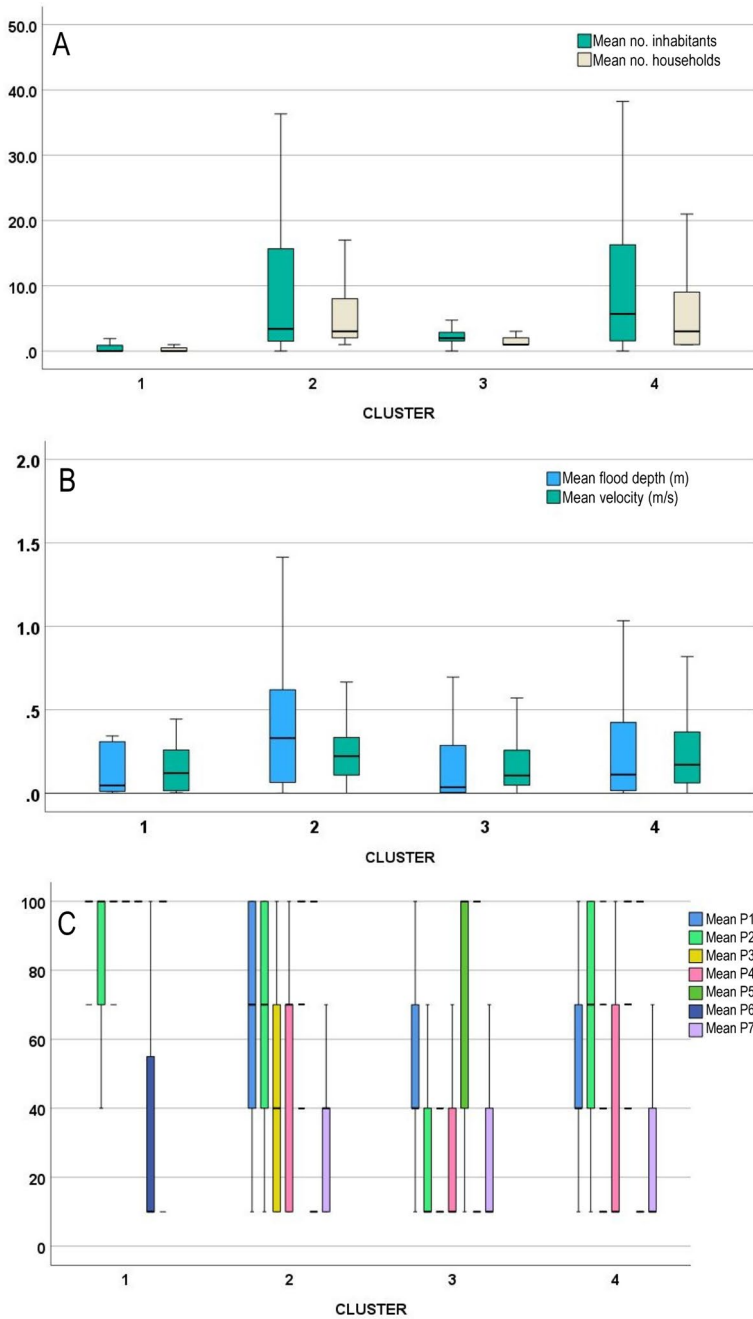


Fig. 7 Clusters of flood hazard and physical vulnerability in the Flood Directive’s areas of significant potential flood risk in the LMA: mean number of exposed population and households per building (A), flood depth and velocity (B), physical vulnerability index and composing parameters P1 to P7 (C). For the location of ASPFR please see Fig. 2

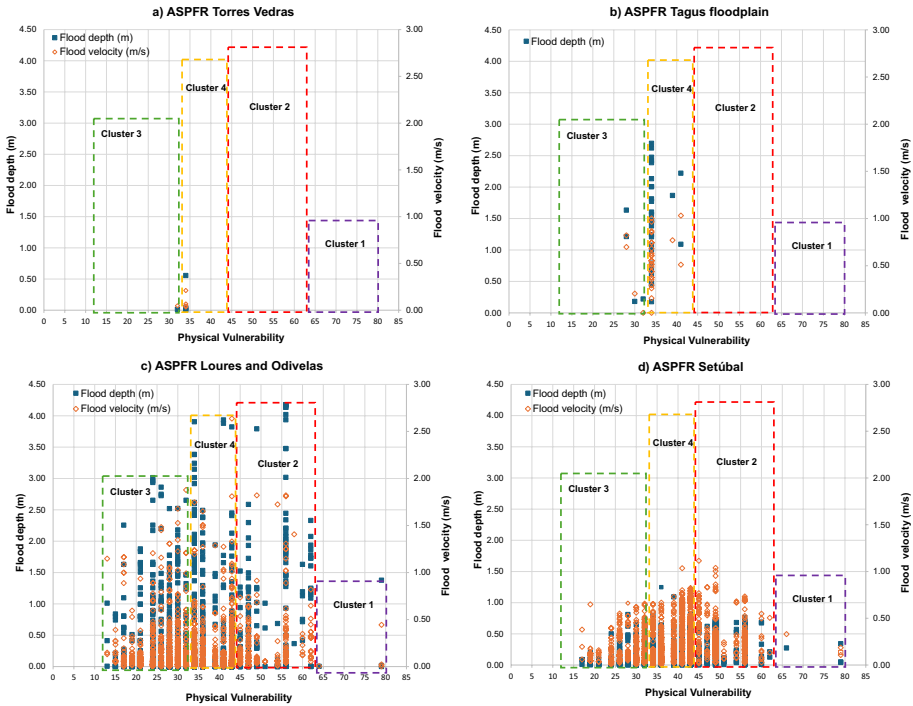


Fig. 8 Distribution of buildings, by cluster membership, in the four ASPFR of the Flood’s Directive in the LMA

The lowest mean vulnerability values are found in cluster 3 for parameters P1, P2, P3 and P4, and for the vulnerability index (26.9) in the critical areas. These results suggest that cluster 3 includes buildings with the lowest index of mean physical vulnerability and hazard variables. Cluster 2 and Cluster 4 present moderate mean values of the vulnerability index (50.8 and 39.2, respectively).

Figure 8 also reveals that the two flood risk areas (ASPFR) located in predominantly urban settings—Loures/Odivelas and Setúbal—exhibit distinct patterns in the relationship between hazard and vulnerability: buildings are generally less vulnerable in the former, though they are subject to higher values of flood height and velocity; in Setúbal, these two flood properties are generally significantly lower. As mentioned above, the Tagus floodplain has the greatest average depth; however, the number of exposed buildings is considerably lower compared to those two mostly urban ASPFR.

Figure 9 expresses the mean values of parameters P1 to P7 in each cluster, aggregating the buildings by ASPFR. In general, the cladding material (P3) is the parameter in which scores are lower (mean of 17.6) with most of the buildings presenting tile, ceramic or mosaic (class A) or stone (class B). Except for the Tagus and Torres Vedras ASPFR, where isolated buildings predominate (class D of parameter P6), exposure features a low mean score as well (24.4 in the 4 areas). On the other side, the parameters of Phys. V in which the buildings perform worse are:

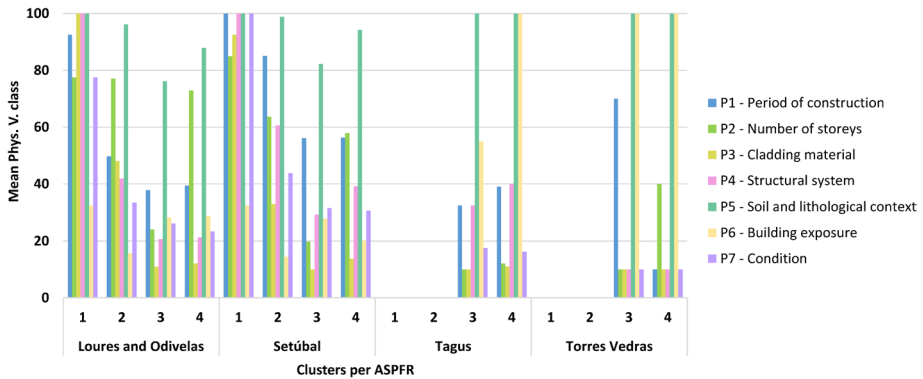


Fig. 9 Physical vulnerability parameters in the Flood Directive's ASPFR

- Regarding parameter P5—soil and lithological context, which comes as non-surprisingly. ASPFR express areas in which exposure and flood susceptibility overlap spatially, with this later being predominantly found in class D of this parameter (alluvial deposits). In the set of the 4 ASPFR, the mean score of P5 is 88.7, with all the buildings of Tagus and Torres Vedras being located on that lithological type. The mean scores in Loures and Odivelas (84.2) and Setúbal (92.5) are equally of concern to the structural stability of buildings;
- Concerning the age-related parameter (P1), which presents the highest mean scores (52.3), it is particularly high in clusters 1 and 2 in Loures and Odivelas and Setúbal ASPFR;
- Concerning parameter P2—number of storeys—whose mean score is 50.9, being particularly high in the most urbanized areas Setúbal and Loures and Odivelas, where buildings are also taller, aggregated in clusters 1 and 2, as well.

Loures and Odivelas recorded the highest physical vulnerability mean values of the cladding materials and structure, while Setúbal recorded the highest physical vulnerability mean values for the building's age and structure.

5 Discussion

A precise assessment of the structural characteristics of buildings to the effect of extreme natural processes causing damage is a thorough, data- and time-intensive task, as it requires intensive fieldwork. Unlike other natural hazards, flood processes are spatially restricted along stream courses and respective bedforms and floodplains, in areas identifiable by local analysis of conditioning factors such as relief, slope, permeability, and erosional and depositional processes and forms (Brierley and Fryirs 2004). This is observed in Fig. 4 and quantified in Table 4, where it is observed that except for a few municipalities, the majority of them feature only a very small fraction of buildings in flood susceptible areas (less or around 1%) and even less in the Flood Directive's ASPFR. Even so, conducting a field-based collection of physical vulnerability-related data on the 2766 buildings would be a costly task.

These two initial considerations (about the vulnerability and the hazard) combine to introduce the value of extensive and regularly collected data sources, like Census data. The applied methodology led to the identification of buildings based on recognized parameters that infer their proneness to suffer structural damage, without fieldwork. Despite this gap—no fieldwork—the fact that the scoring and weighting of parameters and classes are based on laboratory and empirical evidence from past flood impacts provides a relative validation of the resulting indices. Crossing the Phys. V. with the Flood’s Directive and the LMA’s hazardous areas allows us to identify other flood-prone zones where vulnerability would not be neglectable, that were eventually missed out on initial assessments. This is one of the advantages of the method. When a down-scale to the ASPFR is done, other results emerge as useful in flood risk management and particularly in flood adaptation. Building-level measures like retrofitting require a priori knowledge of detailed hazard characteristics like flood depth and velocity, which are specific to flash or progressive floods.

Additionally, the studies elaborated in support of the risk assessment for the 2nd cycle of the Floods’ Directive estimated, under the RCP 4.5 and RCP 8.5 climate change scenarios, increases of 6% from the current 100-year flood peak in the Torres Vedras, Tagus and Loures/Odivelas ASPFR, and 3% for the Setúbal ASPFR. Such context means that, if a reduction in residential areas isn’t imposed by spatial planning instruments, more buildings and inhabitants will be summed up to the figures in Table 4, and existing buildings will be affected by higher flood heights.

Variations in flood depth and velocity along the floodplains express different degrees of loss to buildings. However, few experimental tests exist on the relationship between those components: hazard and building characteristics (Lazzarin et al. 2022). Tailored interventions to deal with flood hazard require a deeper knowledge of the role of depth and velocity as conditioning factors in flood adaptation for spatial planning and house retrofitting. The degree to which the principles of living with floods—or “welcoming” them (Hobeica and Santos 2016)—and reaching “fair” flood risk management (Johnson et al. 2007; Hansson et al. 2008) are a function of our ability to model the benefits of each measure, and particularly in respect to this study, retrofitting at the building level. While most of the LMA’s ASPFR face flash floods, the Tagus one is subject to progressive flooding. About this later, where velocity is normally low in the over banks, a historical adaptation based on stilt-supported construction (and its more recent development as amphibious or floating houses, e.g., English et al. 2016; Moon 2015) has been proven efficient for residential and other uses in dealing with well-known and expected slow onset floods (Mónica Silva et al. 2012). Models such as those discussed by Molinari et al. (2020) are valuable tools to help decide which adaptation measures are better suited for each type of flood. Flood disaster forensic studies (Kreibich et al. 2017; Merz et al. 2021; JRC 2015) and numerical and physical models that consider the flow intrusion on buildings (Mignot and Dewals 2022) provide data that help validate damage functions as well as the efficiency of previously adopted measures.

Endendijk et al. (2022) analyzed the impact of both emergency and structural measures that Netherland residents had taken at the time of the disastrous 2021 flash floods caused by the weather system ‘Bernd’ (Mohr et al. 2023). Their survey concluded that structural interventions like strengthening foundations and using water-resistant materials and floors were efficient in reducing the properties’ damage rations regarding those who haven’t taken measures. In the highly affected Arh Valley, Germany, one year after the event 75.6% of affected residents didn’t plan to relocate, 5.9% were in the relocation process and only 14% have effectively relocated (Truedinger et al. 2023), which means that rationally the residents are willing to cope with future floods, authorities as well and, as a result, houses must

be adapted accordingly. These findings also suggest the need to invest in social vulnerability reduction and resilience strengthening (de Bruijn et al. 2022).

6 Conclusions

In this paper, we presented a simple methodology to evaluate the physical vulnerability of buildings based solely on Census and lithological data. Age, number of storeys and the geological context are the vulnerability factors that most increase the Phys. V. index, while the material of external cladding and the existence of terraced buildings reduce exposure to flood damages and physical vulnerability.

The finding from cluster analysis shows that hazard characteristics and buildings' physical vulnerability combine in diverse patterns. Within exposed buildings, not all are equally vulnerable or exposed to the same flood impact. Cluster 3 was found to be the one with lower risk, while cluster 1 presents the highest vulnerability, however, under low hazard scenarios.

The research highlights the value of Census data at the building level in performing expedited physical vulnerability assessments in vast areas, not requiring fieldwork. The vulnerability results were later combined with local flood hazard resulting from hydraulic modelling. With the increasing availability of global hydrologic-hydraulic models, the proposed clustering method can be extended to the regional or country-level, in support of prioritization of relocation and/or building adaptation to floods.

Author contributions All authors contributed to the study's conception and design. Material preparation and data collection were performed by Pedro Pinto Santos, Susana Pereira, Eusébio Reis, José Luís Zêzere and Tiago Miguel Ferreira. Data analysis was performed by all authors under specific components of flood risk (susceptibility, exposure and vulnerability). The first draft of the manuscript was written by Pedro Pinto Santos, Susana Pereira and Tiago Miguel Ferreira and all authors commented on previous versions of the manuscript. All authors read and approved the final manuscript.

Funding Open access funding provided by FCTIFCCN (b-on). This work was funded by FCT—Portuguese Foundation for Science and Technology, I.P., through the project “MIT-RSC – Multi-risk interactions towards resilient and sustainable cities” [MIT-EXPL/CS/0018/2019].

Declarations

Conflict of interest The authors declare that they have no conflict of interest.

Open Access This article is licensed under a Creative Commons Attribution 4.0 International License, which permits use, sharing, adaptation, distribution and reproduction in any medium or format, as long as you give appropriate credit to the original author(s) and the source, provide a link to the Creative Commons licence, and indicate if changes were made. The images or other third party material in this article are included in the article's Creative Commons licence, unless indicated otherwise in a credit line to the material. If material is not included in the article's Creative Commons licence and your intended use is not permitted by statutory regulation or exceeds the permitted use, you will need to obtain permission directly from the copyright holder. To view a copy of this licence, visit <http://creativecommons.org/licenses/by/4.0/>.

References

Agliata R, Bortone A, Mollo L (2021) Indicator-based approach for the assessment of intrinsic physical vulnerability of the built environment to hydro-meteorological hazards: review of indicators and example

- of parameters selection for a sample area. *Int J Disaster Risk Reduct* 58(March):102199. <https://doi.org/10.1016/j.ijdrr.2021.102199>
- Alfieri L, Bisselink B, Dottori F, Gustavo Naumann Ad, de Roo P, Salamon KW, Feyen L (2017) Global projections of river flood risk in a warmer world. *Earth's Future* 5(2):171–182. <https://doi.org/10.1002/2016EF000485>
- Alfieri L, Dottori F, Betts R, Salamon P, Feyen L (2018) Multi-model projections of river flood risk in Europe under global warming. *Climate*. <https://doi.org/10.3390/cli6010006>
- APA (2014) *Elaboração de cartografia específica sobre o risco de inundação para Portugal Continental*, vol 1
- Arrighi C, Brugiioni M, Castelli F, Franceschini S, Mazzanti B (2018) Flood risk assessment in art cities: the exemplary case of Florence (Italy). *J Flood Risk Manag*. <https://doi.org/10.1111/jfr3.12226>
- Arrighi C, Mazzanti B, Pistone F, Castelli F (2020) Empirical flash flood vulnerability functions for residential buildings. *SN Appl Sci* 2:904. <https://doi.org/10.1007/s42452-020-2696-1>
- Aven T, Renn O (2010) Risk management and governance: concepts, guidelines and applications. *Risk Governance and Society*. <https://doi.org/10.1007/978-3-642-13926-0>
- Ballais JL, Chave S, Dupont N, Masson É, Penven M-J (2011) La méthode hydrogéomorphologique de détermination des zones inondables
- Brierley GJ, Fryirs KA (2004) *Geomorphology and river management: applications of the river styles framework*. Blackwell Publishing, Oxford. <https://doi.org/10.1002/9780470751367>
- Carisi F, Schröter K, Domeneghetti A, Kreibich H, Castellari A (2018) Development and assessment of uni- and multivariable flood loss models for Emilia-Romagna (Italy). *Nat Hazards Earth Syst Sci* 18:2057–2079. <https://doi.org/10.5194/nhess-18-2057-2018>
- Choi HI (2019) Assessment of aggregation frameworks for composite indicators in measuring flood vulnerability to climate change. *Sci Rep* 9(1):1–14. <https://doi.org/10.1038/s41598-019-55994-y>
- D'Ayala D, Wang K, Yan Y, Smith H, Massam A, Filipova V, Pereira JJ (2020) Flood vulnerability and risk assessment of urban traditional buildings in a heritage district of Kuala Lumpur, Malaysia. *Nat Hazard* 20(8):2221–2241. <https://doi.org/10.5194/nhess-20-2221-2020>
- de Bruijn KM, Jafino BA, Merz B, Doorn N, Priest SJ, Dahm RJ, Zevenbergen C, Aerts J CJH, Comes T (2022) Flood risk management through a resilience lens. *Commun Earth Environ* 3(1):8–11. <https://doi.org/10.1038/s43247-022-00613-4>
- de Moel H, Jongman B, Kreibich H, Merz B, Penning-Rowsell E, Ward PJ (2015) Flood risk assessments at different spatial scales. *Mitig Adapt Strat Glob Change* 20(6):865–890. <https://doi.org/10.1007/s11027-015-9654-z>
- Díez-Herrero A, Laín-Huerta L, Lorente-Isidro M (2009) A handbook on flood hazard mapping methodologies. Researchgate.Net. <http://www.igme.es/Publicaciones/publiFree/HandbookFoodHazard/Pdfparadescargar/Ahandbookonfoodhazardmappingtecnologias.pdf>
- Dottori F, Figueiredo R, Martina M, Molinari D, Scorzini AR (2016) INSYDE: a synthetic, probabilistic flood damage model based on explicit cost analysis. *Nat Hazards Earth Syst Sci Discuss*. <https://doi.org/10.5194/nhess-2016-163>
- Endendijk T, Wouter Botzen WJ, De Moel H, Aerts J CJH, Duijndam SJ, Slager K, Kok M (2022) Experience from the 2021 floods in the Netherlands: household survey results on impacts and responses, vol 1
- English E, Klink N, Turner S (2016) Thriving with water: developments in amphibious architecture in North America. In: *FLOODrisk 2016—3rd European conference on flood risk management*, vol 7, p 13009. <https://doi.org/10.1051/e3sconf/20160713009>
- Ferreira TM, Santos PP (2020) An integrated approach for assessing flood risk in historic city centres. *Water (Switzerland)*. <https://doi.org/10.3390/w12061648>
- Gandini A, Egusquiza A, Garmendia L, San-José JT (2018) Vulnerability assessment of cultural heritage sites towards flooding events. *IOP Conf Ser: Mater Sci Eng*. <https://doi.org/10.1088/1757-899X/364/1/012028>
- Garcia RAC, Oliveira SC, Zêzere JL (2016) Assessing population exposure for landslide risk analysis using dasymetric cartography. *Nat Hazards Earth Syst Sci* 12(2769–2782):2016. <https://doi.org/10.5194/nhess-16-2769-2016>
- Hansson K, Danielson M, Ekenberg L (2008) A framework for evaluation of flood management strategies. *J Environ Manag* 86(3):465–480. <https://doi.org/10.1016/j.jenvman.2006.12.037>
- Hobeica L, Santos P (2016) Design with floods: from defence against a 'natural' threat to adaptation to a human-natural process. *Int J Saf Secur Eng* 6(3):616–626. <https://doi.org/10.2495/SAFE-V6-N3-616-626>
- Huang D, Zhang R, Huo Z, Mao F, Youhao E, Zheng W (2012) An assessment of multidimensional flood vulnerability at the provincial scale in China based on the DEA method. *Nat Hazards* 64(2):1575–1586. <https://doi.org/10.1007/s11069-012-0323-1>
- Jacinto R, Grosso N, Reis E, Dias L, Santos FD, Garrett P (2015) Continental Portuguese territory flood susceptibility index—contribution to a vulnerability index. *Nat Hazard* 15(8):1907–1919. <https://doi.org/10.5194/nhess-15-1907-2015>


- Johnson C, Penning-Rowsell E, Parker D (2007) Natural and imposed injustices: the challenges in implementing 'fair' flood risk management policy in England. *Geogr J* 173(4):374–390. <https://doi.org/10.1111/j.1475-4959.2007.00256.x>
- JRC EU expert working group on disaster damage and loss data (2015) Guidance for recording and sharing disaster damage and loss data: towards the development of operational indicators to translate the sendai framework into action. JRC Science and Policy Reports, 28. http://dr.jrc.ec.europa.eu/Portals/0/Loss/JRC_guidelines_loss_data_recording_v10.pdf
- Julià PB, Ferreira TM (2021) From single- to multi-hazard vulnerability and risk in historic urban areas: a literature review: natural hazards, vol 108. Springer, Dordrecht
- Kappes MS, Paphathoma-Köhle M, Keiler M (2012) Assessing physical vulnerability for multi-hazards using an indicator-based methodology. *Appl Geogr* 32(2):577–590. <https://doi.org/10.1016/j.apgeog.2011.07.002>
- Kreibich H, Di Baldassarre G, Vorogushyn S, Aerts JCJH, Apel H, Aronica GT, Arnbjerg-Nielsen K et al (2017) Adaptation to flood risk: results of international paired flood event studies. *Earth's Future* 5(10):953–965. <https://doi.org/10.1002/2017EF000606>
- Laudan J, Rözer V, Sieg T, Vogel K, Thieken AH (2017) Damage assessment in Braunsbach 2016: data collection and analysis for an improved understanding of damaging processes during flash floods. *Nat Hazards Earth Syst Sci* 17:2163–2179. <https://doi.org/10.5194/nhess-17-2163-2017>
- Lazzarin T, Viero DP, Molinari D, Ballio F, Defina A (2022) Flood Damage functions based on a single physics- and data-based impact parameter that jointly accounts for water depth and velocity. *J Hydrol* 607(January):127485. <https://doi.org/10.1016/j.jhydrol.2022.127485>
- Leal M, Ramos C (2013) Susceptibilidade Às Cheias Na Área Metropolitana de Lisboa Norte Factores de Predisposição e Impa Ctes Das Mudanças de Uso Do Solo. *Finisterra* 48(95):17–40. <https://doi.org/10.18055/finis3129>
- Leal M, Reis E, Pereira S, Santos PP (2021) Physical vulnerability assessment to flash floods using an indicator-based methodology based on building properties and flow parameters. *J Flood Risk Manag* 14:1–19. <https://doi.org/10.1111/jfr3.12712>
- Lindersson S, Brandimarte L, Mård J, Di Baldassarre G (2021) Global riverine flood risk—How do hydrogeomorphic floodplain maps compare to flood hazard maps? *Nat Hazards Earth Syst Sci* 21:1–38
- Loureiro JM (2009) Rio Tejo: as grandes cheias 1800–2007. *Tágides*. Vol. 1. Lisbon: Administração da Região Hidrográfica do Tejo I.P. https://apambiente.pt/sites/default/files/_SNIAMB_A_APA/Publicacoes/Tagides/TAGIDES_01.pdf
- Luino F, Turconi L, Petrea C, Nigrelli G (2012) Uncorrected landuse planning highlighted by flooding: the Alba case study (Piedmont, Italy). *Nat Hazards Earth Syst Sci* 12:2329–2346. <https://doi.org/10.5194/nhess-12-2329-2012>
- Marin-Ferrer M, Vernaccini L, Poljansek K (2017) Index for risk management iNFORM concept and methodology report—version 2017. Eur 28655 En
- Mazzoleni M, Mård J, Rusca M, Odongo V, Lindersson S, Di Baldassarre G (2021) Floodplains in the anthropocene: a global analysis of the interplay between human population, built environment, and flood severity. *Water Resour Res* 57(2):e2020WR027744. <https://doi.org/10.1029/2020WR027744>
- Mebarki A, Valencia N, Salagnac JL, Barroca B (2012) Flood hazards and masonry constructions: a probabilistic framework for damage, risk and resilience at urban scale. *Nat Hazards Earth Syst Sci* 12(5):1799–1809. <https://doi.org/10.5194/nhess-12-1799-2012>
- Mejía-Morales MA, Mignot E, Paquier A, Proust S (2023) Laboratory investigation into the effect of the storage capacity of a city block on unsteady urban flood flows. *Water Resour Res* 59(4):e2022WR032984
- Merz B, Blöschl G, Vorogushyn S, Dottori F, Aerts JCJH, Bates P, Bertola M et al (2021) Causes, impacts and patterns of disastrous river floods. *Nat Rev Earth Environ* 2(9):592–609. <https://doi.org/10.1038/s43017-021-00195-3>
- Mignot E, Dewals B (2022) Hydraulic Modelling of inland urban flooding: recent advances. *J Hydrol*. <https://doi.org/10.1016/j.jhydrol.2022.127763>
- Miranda FN, Ferreira TM (2019) A simplified approach for flood vulnerability assessment of historic sites. *Nat Hazards* 96(2):713–730. <https://doi.org/10.1007/s11069-018-03565-1>
- Mohr S, Ehret U, Kunz M, Ludwig P, Caldas-Alvarez A, Daniell JE, Ehmele F et al (2023) A multi-disciplinary analysis of the exceptional flood event of July 2021 in central Europe—part 2: historical context and relation to climate change. *Nat Hazard* 23(4):1287–1311. <https://doi.org/10.5194/nhess-23-1287-2023>
- Molinari D, Scorzini AR, Arrighi C, Carisi F, Castelli F, Domeneghetti A, Gallazzi A et al (2020) Are flood damage models converging to 'reality'? Lessons learnt from a blind test. *Nat Hazard* 20(11):2997–3017. <https://doi.org/10.5194/nhess-20-2997-2020>
- Moon C (2015) A study on the floating house for new resilient living. *J Korean Hous As* 26(5):97–104. <https://doi.org/10.6107/jkha.2015.26.5.097>

- Nasiri H, Yusof MJM, Ali TAM (2016) An overview to flood vulnerability assessment methods. *Sustain Water Resour Manag* 2(3):331–336. <https://doi.org/10.1007/s40899-016-0051-x>
- NATO (2006) Flood risk management: hazards, vulnerability and mitigation measures. Edited by Jochen Schanze, Evzen Zemen, and Jiri Marsalek
- Pereira S, Zêzere JL, Quaresma I, Santos PP, Santos M (2016) Mortality patterns of hydro-geomorphologic disasters. *Risk Anal*. <https://doi.org/10.1111/risa.12516>
- Pereira S, Santos PP, Zêzere JL, Tavares AO, Garcia RAC, Oliveira SC (2020) A landslide risk index for municipal land use planning in Portugal. *Sci Total Environ* 735:139463. <https://doi.org/10.1016/j.scitotenv.2020.139463>
- Postacchini M, Zitti G, Giordano E, Clementi F, Darvini G, Lenci S (2019) Flood impact on masonry buildings: the effect of flow characteristics and incidence angle. *J Fluids Struct* 88:48–70. <https://doi.org/10.1016/j.jfluidstruct.2019.04.004>
- Reis E (2011) Análise de Bacias Hidrográficas, Susceptibilidade à Ocorrências de Cheias e Sistemas de Informação Geográfica: Da Definição Do Quadro Conceptual Até à Proposta de Um Modelo de Avaliação. VIII Congresso Da Geografia Portuguesa, pp 1–6
- Saber M, Abdrabo KI, Habiba OM, Kantosh SA, Sumi T (2020) Impacts of triple factors on flash flood vulnerability in Egypt: urban growth, extreme climate, and mismanagement. *Geosciences* 10(1):24. <https://doi.org/10.3390/geosciences10010024>
- Santos PP, Reis E (2018) Assessment of Stream flood susceptibility: a cross-analysis between model results and flood losses. *J Flood Risk Manag*. <https://doi.org/10.1111/jfr3.12290>
- Santos PP, Reis E, Pereira S, Santos M (2019) A flood susceptibility model at the national scale based on multicriteria analysis. *Sci Total Environ* 667:325–337. <https://doi.org/10.1016/j.scitotenv.2019.02.328>
- Santos PP, Pereira S, Rocha J, Reis E, Santos M, Oliveira SC, Garcia RAC, Melo R, Zêzere JL (2022) The role of susceptibility, exposure and vulnerability as drivers of flood disaster risk at the parish level. *Environ Earth Sci* 81(19):465. <https://doi.org/10.1007/s12665-022-10589-1>
- Shonkoff JP, Richmond JB, Sampson CC, Smith AM, Bates PD, Neal JC, Alfieri L, Freer JE (2015) A high-resolution global flood hazard model. *Water Resour Res* 51(9):7358–7381. <https://doi.org/10.1002/2015WR016954>. Received
- Silva M, Pereira S (2014) Assessment of physical vulnerability and potential losses of buildings due to shallow slides. *Nat Hazards* 72(2):1029–1050. <https://doi.org/10.1007/S11069-014-1052-4/TABLES/3>
- Silva M, Mendonça P, Branco J (2012) Traditional wooden buildings in Portugal—the Avieira house. In: International conference “sustainable environment in the mediterranean region: from housing to urban and land scale construction”, Naples, Italy , no. February: 3–8. c:%5CUsers%5CUuario%5CDesktop%5CPhD%5CPapers%5CSilva M., Mendona P., Branco J. - Traditional wooden buildings in Portugal - The Avieira house.pdf
- Simões AG, Appleton JG, Bento R, Caldas JV, Lourenço PB, Lagomarsino S (2017) Architectural and structural characteristics of masonry buildings between the 19th and 20th centuries in Lisbon, Portugal. *Int J Arch Herit* 11(4):457–474. <https://doi.org/10.1080/15583058.2016.1246624>
- Stephenson V, D’Ayala D (2014) A new approach to flood vulnerability assessment for historic buildings in England. *Nat Hazard* 14(5):1035–1048. <https://doi.org/10.5194/nhess-14-1035-2014>
- Sturm M, Gems B, Keller F, Mazzorana B, Fuchs S, Papathoma-Köhle M, Aufleger M (2018) Experimental analyses of impact forces on buildings exposed to fluvial hazards. *J Hydrol* 565:1–13. <https://doi.org/10.1016/j.jhydrol.2018.07.070>
- Truedinger AJ, Jamshed A, Sauter H, Birkmann J (2023) Adaptation after extreme flooding events: moving or staying? The case of the Ahr Valley in Germany. *Sustainability* 15(2):1407. <https://doi.org/10.3390/su15021407>
- Vojtek M, Vojteková J, Luca DLD, Petroselli A (2023) Combined basin-scale and decentralized flood risk assessment: a methodological approach for preliminary flood risk assessment. *Hydrol Sci J* 00(00):1–24. <https://doi.org/10.1080/02626667.2022.2157279>
- Wagenaar D, De Jong J, Bouwer LM (2017) Multi-variable flood damage modelling with limited data using supervised learning approaches. *Nat Hazards Earth Syst Sci* 17:1683–1696. <https://doi.org/10.5194/nhess-17-1683-2017>
- WBGU (2000) Strategies for managing global environmental risks world in transition: strategies for managing global environmental risks
- Wing OEJ, Bates PD, Smith AM, Sampson CC, Johnson KA, Fargione J, Morefield P (2018) Estimates of present and future flood risk in the conterminous United States. *Environ Res Lett* 13:3. <https://doi.org/10.1088/1748-9326/aaac65>
- Wisner B, Blaikie P, Cannon T, Davis I (2004) At risk: natural hazards, peoples vulnerability and disasters, 2nd edn. Routledge, London
- Xofi M, Ferreira TM, Domingues JC, Santos PP, Pereira S, Oliveira SC, Reis E, Zêzere JL, Garcia RAC, Lourenço PB (2023) On the seismic vulnerability assessment of urban areas using census data: the Lisbon metropolitan area as a pilot study area. *J Earthq Eng* 00(00):1–24. <https://doi.org/10.1080/13632469.2023.2197078>

- Zahmatkesh Z, Karamouz M (2017) An uncertainty-based framework to quantifying climate change impacts on coastal flood vulnerability: case study of New York City. *Environ Monit Assess* 189:11. <https://doi.org/10.1007/s10661-017-6282-y>
- Zêzere JL, Pereira S, Tavares AO, Bateira C, Trigo RM, Quaresma I, Santos PP, Santos M, Verde J (2014) DISASTER: a GIS database on hydro-geomorphologic disasters in Portugal. *Nat Hazards* 72:2. <https://doi.org/10.1007/s11069-013-1018-y>
- Zêzere JL, Vaz T, Pereira S, Oliveira SC, Marques R, Garcia RAC (2015) Rainfall thresholds for landslide activity in Portugal: a state of the art. *Environ Earth Sci* 73(6):2917–2936. <https://doi.org/10.1007/s12665-014-3672-0>

Publisher's Note Springer Nature remains neutral with regard to jurisdictional claims in published maps and institutional affiliations.

Authors and Affiliations

Pedro Pinto Santos^{1,2}  · Susana Pereira^{1,3} · José Luís Zêzere^{1,2} · Eusébio Reis^{1,2} · Sérgio Cruz Oliveira^{1,2} · Ricardo A. C. Garcia^{1,2} · Tiago Miguel Ferreira⁴

✉ Pedro Pinto Santos
pmpsantos@edu.ulisboa.pt

Susana Pereira
sspereira@letras.up.pt

José Luís Zêzere
zezere@edu.ulisboa.pt

Eusébio Reis
eusebioreis@edu.ulisboa.pt

Sérgio Cruz Oliveira
cruzdeoliveira@edu.ulisboa.pt

Ricardo A. C. Garcia
rgarcia@edu.ulisboa.pt

Tiago Miguel Ferreira
Tiago.Ferreira@uwe.ac.uk

¹ Centre of Geographical Studies, Institute of Geography and Spatial Planning, University of Lisbon, Lisbon, Portugal

² Associate Laboratory TERRA, University of Lisbon, Lisbon, Portugal

³ Centre of Studies in Geography and Spatial Planning, Geography Department, Faculty of Arts and Humanities, University of Porto, Porto, Portugal

⁴ College of Arts, Technology and Environment - School of Engineering, University of the West of England (UWE Bristol), Bristol, UK